

# On-chip separation of *Lactobacillus* bacteria from yeasts using dielectrophoresis

Khashayar Khoshmanesh · Sara Baratchi · Francisco J. Tovar-Lopez · Saeid Nahavandi · Donald Wlodkovic · Arnan Mitchell · Kourosh Kalantar-zadeh

Received: 4 October 2011 / Accepted: 25 October 2011 / Published online: 11 November 2011  
© Springer-Verlag 2011

**Abstract** Dielectrophoresis, the induced motion of dielectric particles in non-uniform electric fields, enables the separation of suspended bio-particles based on their dimensions or dielectric properties. This work presents a microfluidic system, which utilises a combination of dielectrophoretic (DEP) and hydrodynamic drag forces to separate *Lactobacillus* bacteria from a background of yeasts. The performance of the system is demonstrated at two operating frequencies of 10 MHz and 100 kHz. At 10 MHz, we are able to trap the yeasts and bacteria at different locations of the microelectrodes as they experience different magnitudes of DEP force. Alternatively, at 100 kHz we are able to trap the bacteria along the microelectrodes, while repelling the yeasts from the microelectrodes and washing them away by the drag force. These separation mechanisms might be applicable to automated lab-on-a-chip systems for the rapid and label-free separation of target bio-particles.

**Keywords** Dielectrophoresis · Microfluidics · Cell · Bacteria · Sorting

## 1 Introduction

Early detection and isolation of bacteria (prokaryote cells) from eukaryotic cells is essential for the diagnosis of bacterial infections and food contaminations. There are a variety of techniques to detect bacterial infections in clinical laboratories. Those include (i) conventional staining such as gram-stain, acid-fast stain and immunofluorescence; (ii) cultural and biochemical methods; (iii) antibody-based methods such as enzyme-linked immunosorbent assay (ELISA), Western blotting (WB), complement fixation test and particle agglutination; and (iv) molecular-based methods such as polymerase chain reaction (PCR), and real-time PCR.

Microfabricated, microfluidic systems are widely considered as an enabling technology in microbiology. Low cell numbers, small reagent volumes, fast mass transfer kinetics and rapid reaction times in the microfabricated environments provide the unique ability to monitor bacterial infections, especially in low concentrations. In this context, a large number of emerging technologies have been reported for the detection and separation of bacterial samples in microfabricated systems, including flow fraction (Mach and Di Carlo 2010), bio-luminescence (Qiu et al. 2009), surface plasmon resonance (Mazumdar et al. 2010), magnetic field gradient (Xia et al. 2006), electrical impedance spectroscopy (Yang 2008), isotachopheresis (Bercovici et al. 2011; Persat and Santiago 2011) and dielectrophoresis (Lapizco-Encinas et al. 2004).

Dielectrophoresis, the induced motion of polarisable particles in a non-uniform electric field, in particular, can

---

K. Khoshmanesh (✉) · S. Nahavandi  
Centre for Intelligent Systems Research, Deakin University,  
Geelong, VIC 3217, Australia  
e-mail: khashayar.khoshmanesh@deakin.edu.au;  
kh\_khoshmanesh@yahoo.com

S. Baratchi  
Department of Biochemistry and Molecular Biology,  
Monash University, Melbourne, VIC 3800, Australia

F. J. Tovar-Lopez · A. Mitchell · K. Kalantar-zadeh  
School of Electrical and Computer Engineering,  
RMIT University, Melbourne, VIC 3001, Australia

D. Wlodkovic  
The BioMEMS Research Group, School of Chemical Sciences,  
University of Auckland, Auckland 1142, New Zealand

selectively and accurately push the suspended bio-particles towards or away from the microelectrodes (positive/negative dielectrophoresis) (Pethig 2010; Kang and Li 2009). Dielectrophoresis has been widely applied in microfluidic systems to manipulate, transport, separate and characterise bio-particles, including multicellular organisms (Khoshmanesh et al. 2011b), mammalian cells (Khoshmanesh et al. 2011a; Kang et al. 2008), bacteria (Hu et al. 2005), viruses (Park et al. 2007) and cell organelles (Moschallski et al. 2010), as comprehensively reviewed in (Khoshmanesh et al. 2011c; Pethig 2010).

Most DEP systems take advantage of metallic microelectrodes that are patterned on glass or silicon substrates to create non-uniform electric fields within a microenvironment. Wang et al. (1993) were one of the first to separate bacteria from blood samples using metallic microelectrodes. Similar systems have been applied by others for the separation of bacteria from a solution containing beads (Moon et al. 2009), and the separation of live and heat-treated bacteria (Li and Bashir 2002). Alternatively, electrodeless DEP systems have been introduced to eliminate the operational issues associated with metallic microelectrodes such as corrosion and undesired electrochemical reactions, which happen on the surface of the microelectrodes at lower frequencies and high medium conductivities. Lapizco-Encinas et al. (2004) applied insulating posts to separate bacterial samples suspended in the flow. Cho et al. (2009) integrated a polymer membrane containing conical nanopores into a microchannel to concentrate bacteria inside the pores. More recently, Jaramillo et al. utilised 3-D carbon microelectrodes to trap and release bacteria (del Carmen Jaramillo et al. 2010).

Moreover, different operating strategies have been applied to improve the DEP systems. Markx et al. (1996) demonstrated the temporal variation of medium conductivity for the selective separation of bacteria. The bacteria were first trapped at the microelectrodes under positive dielectrophoresis, and the conductivity of the medium was gradually increased to release the bacteria according to their dielectric properties. Hu et al. (2005) applied a marker-specific sorting strategy, in which target bacteria were labelled with polymeric beads to be separated from a background of non-labelled bacteria. The labelled bacteria had a much larger dimension compared to non-labelled ones and could be deflected towards the collection channel under negative dielectrophoresis. Zhou et al. (2006) utilised single-walled carbon nanotubes to enhance the DEP mobility and trapping of bacteria. Koo et al. (2009) used antigen–antibody reactions to separate bacteria. Antibody molecules were patterned on the surface of the microchannel. The bacteria were pushed towards the microelectrode gaps under positive dielectrophoresis and brought into contact with the antibodies.

In this work, we present the DEP separation of *Lactobacillus acidophilus* bacteria from a background of *Saccharomyces cerevisiae* yeasts suspended in an isotonic buffer with an electrical conductivity of 0.025 S/m. The core of the system is an array of curved microelectrodes that are patterned on a glass substrate. The performance of the system is assessed by separating bacteria from yeasts. The experiments are conducted at two distinct scenarios. First, the frequency of the applied AC signal is set to 10 MHz, at which both bio-particles demonstrate positive DEP response and are pushed towards the microelectrodes. However, the yeasts experience a much stronger DEP force due to their larger dimensions and are mostly trapped at the entrance region of microelectrodes, while the bacteria are mostly trapped at the tip region. Second, the frequency is set to 100 kHz, at which the bacteria demonstrate positive DEP response and are trapped at the microelectrodes, while the yeasts demonstrate negative DEP response and are repelled from the microelectrodes to be washed away by the flow. The current DEP system offers the rapid and label-free detection of bacterial infections in biological samples. It avoids extensive preparation procedures and can be readily integrated into other microfluidic components.

## 2 Theoretical background

The motion of yeasts and *Lactobacillus* bacteria is governed by the interaction of three forces: DEP force which pushes the bio-particles towards or away from the microelectrodes, sedimentation force which pushes the bio-particles downward, and finally the hydrodynamic drag force which pushes the bio-particles through the microchannel and resists against any change of direction.

Yeasts have an ellipsoidal shape with a principal diameter of  $\sim 9 \mu\text{m}$ , and semi-principal diameters ranging from 6 to 8  $\mu\text{m}$ . However, in most DEP studies, the yeasts are considered as spherical structures (Huang et al. 1992) with an average diameter of  $\sim 8 \mu\text{m}$ . Under this assumption, the time-averaged DEP, hydrodynamic drag and sedimentation forces applied on yeasts were derived as (Pethig 2010):

$$\bar{F}_{\text{DEP-cell}} = 2\pi r^3 \varepsilon_{\text{medium}} \text{Re}[f_{\text{CM-cell}}] \nabla E_{\text{rms}}^2 \quad (1)$$

$$F_{\text{Drag-cell}} = 6\pi r \mu (\vec{U}_x - \vec{v}_{\text{cell}}) \quad (2)$$

$$F_{\text{Sedimentation-cell}} = \frac{4}{3} \pi r^3 (\rho_{\text{cell}} - \rho_{\text{medium}}) \vec{g}_z \quad (3)$$

In Eq. 1,  $r$  is the radius of the yeasts,  $\varepsilon$  is the permittivity,  $E_{\text{rms}}$  is the root-mean square (rms) value of the applied electric field, and  $\text{Re}[f_{\text{CM}}]$  is the real part of the

Clausius–Mossotti (CM) factor, representing the polarisation of yeasts with respect to the surrounding medium. In Eq. 2,  $\mu$  is the dynamic viscosity of the medium,  $\vec{U}_x$  is the velocity of the suspending medium, and  $\vec{v}$  is the velocity of the yeasts. Finally in Eq. 3,  $\rho$  is the density, and  $\vec{g}_z$  is the gravitational acceleration.

Alternatively, the *Lactobacillus acidophilus* bacteria have a cylindrical shape with hemispherical ends with a diameter of 0.6–0.9  $\mu\text{m}$  and a height of  $\sim 1.5 \mu\text{m}$ . However, in most DEP studies the bacteria are considered as ellipsoid structures (Castellarnau et al. 2006). Under this assumption, the time-averaged DEP, hydrodynamic drag and sedimentation forces applied on bacteria were derived as (Pethig 2010):

$$\bar{F}_{\text{DEP-bacteria}} = \frac{\pi}{3} r^2 L \epsilon_{\text{medium}} \text{Re}[f_{\text{CM-bacteria}}] \nabla E_{\text{rms}}^2 \quad (4)$$

$$F_{\text{Drag-bacteria}} = \frac{6\pi r \mu}{\ln(r/L)} (\vec{U}_x - \vec{v}_{\text{bacteria}}) \quad (5)$$

$$F_{\text{Sedimentation-bacteria}} = \frac{4}{3} \pi r^2 L (\rho_{\text{bacteria}} - \rho_{\text{medium}}) \vec{g}_z \quad (6)$$

In Eq. 4,  $L$  and  $2r$  are the diameter of the bacteria along its major and minor axes, respectively (Fig. 1).

The motion of yeasts and bacteria under the combined influence of DEP, hydrodynamic drag and sedimentation forces can be obtained by solving the Newton’s second law of motion:

$$\bar{F}_{\text{DEP}} + F_{\text{Drag}} + F_{\text{Sedimentation}} = m\vec{a} \quad (7)$$

where  $\vec{a}$  is the acceleration of bio-particles. Substituting the Eqs. 1–6 in the above equation leads to a second-order

differential equation, from which the velocity of bio-particles is obtained as below:

$$\vec{v}_{\text{cell}} \approx \frac{r^2 \epsilon_{\text{medium}} \text{Re}[f_{\text{CM-cell}}] \nabla E_{\text{rms}}^2}{3\mu} + \vec{U}_x + \frac{2}{9} \frac{r^2 (\rho_{\text{cell}} - \rho_{\text{medium}}) \vec{g}_z}{\mu} \quad (8)$$

$$\vec{v}_{\text{bacteria}} \approx \frac{rL \ln\left(\frac{r}{L}\right) \epsilon_{\text{medium}} \text{Re}[f_{\text{CM-bacteria}}] \nabla E_{\text{rms}}^2}{18\mu} + \vec{U}_x + \frac{2}{9} \frac{rL \ln\left(\frac{r}{L}\right) (\rho_{\text{bacteria}} - \rho_{\text{medium}}) \vec{g}_z}{\mu} \quad (9)$$

Equations 8–9 comprise three terms corresponding to DEP, drag and sedimentation forces, respectively. The DEP term depends on  $\nabla E_{\text{rms}}^2$  and  $\text{Re}[f_{\text{CM}}]$ , which need to be calculated. The  $\nabla E_{\text{rms}}^2$  depends on the configuration of microelectrodes and the magnitude of AC signal, and can be obtained by numerical simulations (Khoshmanesh et al. 2010b). On the other hand, the  $\text{Re}[f_{\text{CM}}]$  depends on the dielectric properties of bio-particles and the suspending medium and also the frequency of the AC signal. The  $f_{\text{CM-cell}}$  was calculated using the spherical double-shell model, in which the yeasts were considered as spherical structures, comprising cell interior, plasma membrane and an outer wall (Huang et al. 1992) (see Appendix). Alternatively, the  $f_{\text{CM-bacteria}}$  was calculated using the ellipsoid double-shell model, in which the bacteria were considered as ellipsoid structures comprising cytoplasm, plasma membrane and an outer wall (Castellarnau et al. 2006) (see Appendix).

Figure 1 shows the variations of  $\text{Re}[f_{\text{CM}}]$  for yeasts and *Lactobacillus* bacteria at different frequencies of 1 kHz to 25 MHz when the bio-particles are dispersed in an isotonic buffer with an electrical conductivity of 0.025 S/m. Considering yeasts as spherical structures with a diameter of 8  $\mu\text{m}$ , they demonstrated a crossover frequency of 225 kHz, as confirmed by experiments, beyond which they exhibited positive DEP response. The  $\text{Re}[f_{\text{CM}}]$  reached a minimum of  $-0.446 \pm 0.07$  at frequencies less than 30 kHz while reaching a maximum of  $0.464 \pm 0.027$  at 1–9.25 MHz range. Interestingly, considering yeasts as ellipsoidal structures with a principal diameter of 9  $\mu\text{m}$ , and semi-principal diameters of 6  $\mu\text{m}$  did not alter the crossover frequency, but led to a stronger DEP response along the principal axis (Fig. 1).

In contrast, the bacteria demonstrated a positive DEP response at the entire frequency range along their L-axis, as confirmed by experiments (Fig. 1). The  $\text{Re}[f_{\text{CM}}]$  remained almost constant at  $0.18 \pm 0.01$  at frequencies less than the 250 kHz range, while reaching a sharp peak of 0.869 at 5.5 MHz. The separation of bacteria from yeasts was conducted at two frequencies of 100 kHz and 10 MHz to take advantage of the highest distinction between the DEP response of yeast and bacteria, as shown by arrows.

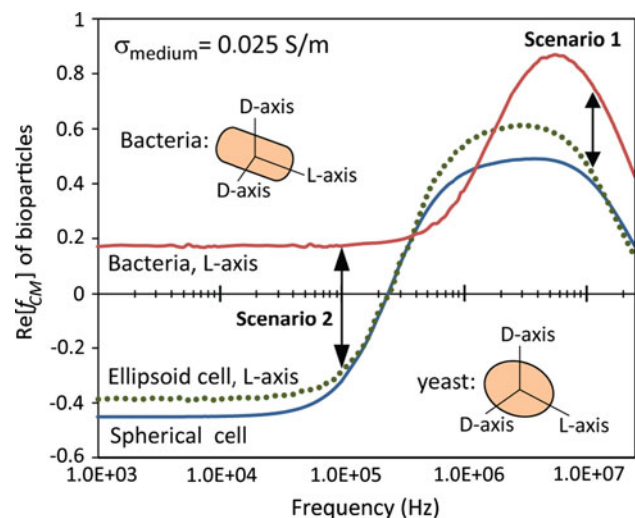


**Fig. 1** Variations of  $\text{Re}[f_{\text{CM}}]$  for yeasts and *Lactobacillus* bacteria at  $\sigma_{\text{medium}} = 0.025 \text{ S/m}$ , revealing the positive DEP response of yeasts at frequencies higher than 225 kHz and of bacteria throughout the entire frequency spectrum

### 3 Materials and methods

#### 3.1 Principles of the DEP system

Figure 2a presents the plane view of the current DEP system. The system comprises a microchannel that is integrated onto a glass substrate. The microchannel is fabricated from poly-dimethylsiloxane (PDMS) with a width of 600  $\mu\text{m}$  and a thickness of 80  $\mu\text{m}$ . The substrate is a glass slide of  $75 \times 25.5 \times 1$  mm that supports five pairs of microelectrodes on its surface. The electric potential is applied through the pads of  $6 \times 2.25$  mm patterned on both sides of the microchannel. The microelectrodes have a curved configuration with a width of 50  $\mu\text{m}$  and a gap of 1,000  $\mu\text{m}$  between the consequential pairs. The gap between the opposite microelectrodes reduces continuously until it reaches 40  $\mu\text{m}$  at the centreline of the microchannel. The curved microelectrodes create a strong spatially varying electric field within the microchannel, which is crucial to create dielectrophoresis. The curved microelectrodes have distinct advantages over other configurations, as reported in (Khoshmanesh et al. 2011c; Khoshmanesh et al. 2010b). They generate a strong electric field and maintain it over a large portion of their structure. The induced electric field increases very smoothly along the structure and therefore the particles do not experience undesired motions over the tips (Khoshmanesh et al. 2010b).

#### 3.2 Fabrication process

To fabricate the DEP platform, thin films of chrome/gold were deposited on the surface of glass substrates using the electron beam evaporation process with a thickness of 500/1,500  $\text{\AA}$ , respectively. The microelectrodes were patterned using lithography. A thin film of AZ1512 (Clariant, USA)

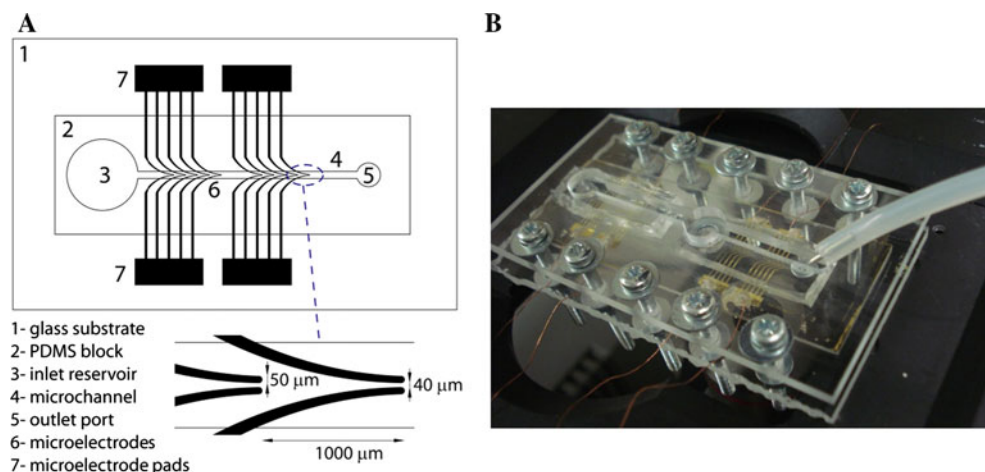
positive photoresist was spin coated on the substrate at a thickness of 1  $\mu\text{m}$ . The sample was exposed to UV light using a mask aligner (Karl Suss MA6) and then developed. Finally, the additional chrome/gold film was etched using etching solutions.

Similarly, the microchannel was made from PDMS using lithography. A 3-inch diameter silicon wafer was used as the substrate and spin coated with KMPP (MicroChem Corporation) negative photoresist to a thickness of 80  $\mu\text{m}$ . The sample was exposed to UV light using the MA6 mask aligner and developed with an SU-8 developer. PDMS (SYLGARD 184, Dow Corning) was poured onto the master to realise the microchannel. The resulting PDMS microchannel was assembled on the DEP platform. Copper wires were bounded to the microelectrode pads using silver-based epoxy glue and baked in an oven. The DEP system was then sandwiched between two polymethyl methacrylates (PMMA) coverslips to avoid leakage, as shown in Fig. 2b.

#### 3.3 Sample preparation

Instant dried yeast powder (Tandaco, NSW, Australia) was used as the source of *Saccharomyces cerevisiae* yeasts. To prepare the yeast suspension, 40 mg of yeast powder was mixed with 10 ml of phosphate buffer and diluted with an isotonic buffer of distilled water, 8.5% w/v sucrose and 0.3% w/v dextrose (Gascoyne et al. 1997) to obtain an electrical conductivity of 0.025 S/m. After dilution, the initial concentration of yeasts reached  $6\text{--}7 \times 10^7$  cells per ml measured by a standard Neubauer counting chamber. Alternatively, Inner Health Plus capsules (Health World Limited, Queensland, Australia) were used as the source of *Lactobacillus* bacteria. Similarly, to prepare the bacterial suspension, 40 mg of capsule powder was mixed with 10 ml of phosphate buffer and diluted with the same isotonic buffer

**Fig. 2** **a** The layout of the DEP system, comprising a PDMS microchannel integrated into a DEP platform. **b** The PDMS blocks were integrated into the DEP platform to make up the DEP system. The shown platform consisted of two separate DEP systems



to obtain an electrical conductivity of 0.025 S/m. After dilution, the initial concentration of bacteria  $1.7\text{--}2.5 \times 10^7$  bacteria per ml was measured by a Petroff Hausser counting chamber.

### 3.4 Experimental setup

During the experiments, the applied suspensions were injected to the inlet reservoir and sucked out from the outlet port at the desired flow rates using a syringe pump (Harvard Apparatus, PHD 2000). The performance of the systems was observed using an inverted optical microscope (Nikon Eclipse, TE 2000-U). An oscillating wave was applied to the electrode pads using a function generator (Tabor Electronics, series 8200). The electrical conductivity of the medium was measured using a high precision conductivity meter (ECTestr11+, Eutech Instruments).

### 3.5 Quantification of trapping and separation efficiencies

The performance of the DEP system was quantified in terms of its trapping efficiency defined as  $(n_{\text{inlet}} - n_{\text{outlet}})/n_{\text{inlet}} \times 100\%$ , where  $n$  is the number of bio-particles, and separation efficiency defined as  $(f_{\text{inlet}} - f_{\text{outlet}})/f_{\text{inlet}} \times 100\%$ , where  $f$  is the fraction of target bio-particles with respect to all particles. The above evaluations were conducted using a Petroff Hausser counting chamber for bacteria and a standard Neubauer counting chamber for yeasts.

To count the number of bacteria, a single drop of the 1:10 diluted sample was applied to the counting chamber and examined using a  $100 \times$  oil immersion objective of the microscope. The number of bacteria was counted in 20 squares of the Petroff Hausser counting chamber, and the total bacteria per millilitre of the suspension was calculated according to the manufacturer's instructions (Treuer and Haydel 2011). The number of bacteria was counted at the inlet and outlet of the DEP system to obtain the values of  $n_{\text{inlet}}$  and  $n_{\text{outlet}}$ . This procedure was repeated three times and the data presented as mean  $\pm$  standard error.

Alternatively, the yeasts were diluted 1:5 and applied to a Neubauer counting chamber. The stained cells were visualised using a  $20 \times$  objective on the microscope. The number of cells was counted in five squares of the hemocytometer, and the total cells per millilitre of the suspension were calculated according to the manufacturer's instructions. The number of cells was counted at the inlet and outlet of the DEP system, to obtain the values of  $n_{\text{inlet}}$  and  $n_{\text{outlet}}$ .

## 4 Results and discussions

The separation of bacteria from yeasts was demonstrated in two distinct scenarios. In both scenarios, a stream of medium was applied through the microchannel with a flow rate of 0.5  $\mu\text{lit}/\text{min}$  (corresponding to an average velocity of 0.017 mm/s), the electrical conductivity of which was adjusted to 0.025 S/m, while the microelectrodes were energised with an AC signal of 15 Vp-p. However, the two scenarios differed in the frequency of the AC signal applied to the microelectrodes. In the first scenario, the frequency was set to 10 MHz, as described in Sect. 4.1, whereas in the second scenario the frequency was set to 100 kHz, as described in Sect. 4.2.

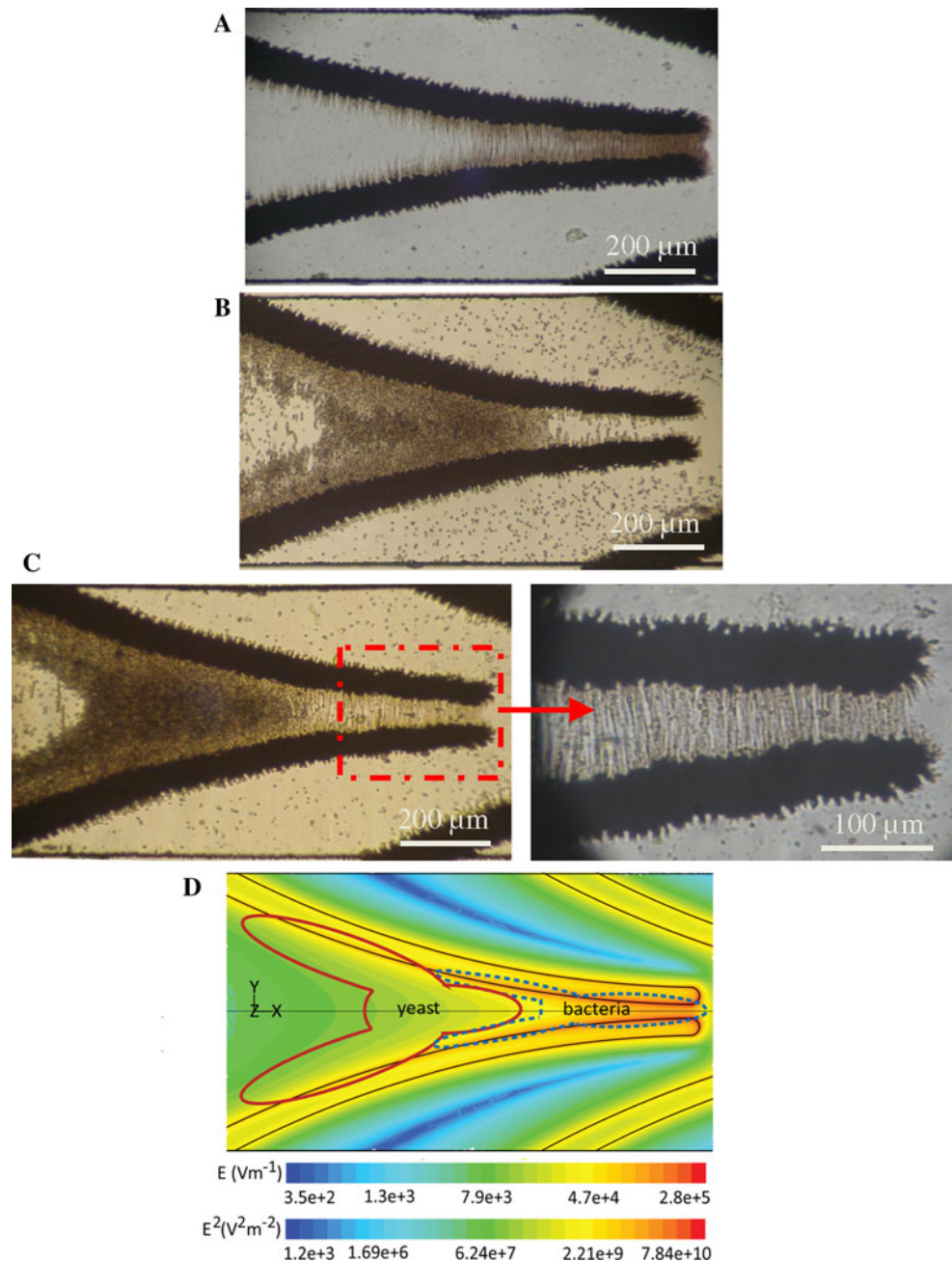
### 4.1 Separation of bacteria from yeasts at 10 MHz

At 10 MHz, both bacteria and yeasts demonstrated positive DEP response (Fig. 1). To understand the mechanism of separation, we first analysed the DEP response of bacteria (Fig. 3a) and yeasts (Fig. 3b) in separate experiments.

Approaching the first microelectrode, the suspended bacteria lost their levitation height under the influence of DEP and sedimentation forces. The rate of height loss is proportional to  $\dot{z} \propto rL \ln(r/L) \text{Re}[f_{\text{CM-bacteria}}] \nabla E_{\text{rms}}^2 / \mu$  for bacteria, as obtained in Sect. 2. The bacteria have a small dimension, and eventually experience a small height loss. This implies that the bacteria which were moving close to the bottom surface were immediately trapped along the microelectrode edges, whereas the ones moving at higher heights were trapped a few microns away at the tip region either due to gradual loss of height or due to the presence of stronger DEP forces. The trapping was initiated with immobilisation of one layer of bacteria along the inner edges of the microelectrode and followed by immobilisation of another layer of bacteria at the free ends of the previous layer to form a long chain along the electric field lines. The density of bacterial chains increased along the microelectrode structure and reached a peak at the tip region (Fig. 3a). Under the applied conditions, most of the bacteria were trapped at the first microelectrode pair, and the density of immobilised bacteria decreased consistently at the consequential pairs.

Alternatively, at the vicinity of the first microelectrode, the neighbouring yeasts become polarised and attached to each other to form the so-called pearl chain at the entrance of the microelectrode. Getting closer to the edges of the microelectrode, the pearl chains were broken; the yeasts lost their height and moved towards the microelectrodes. The rate of height loss is proportional to  $\dot{z} \propto r^2 \text{Re}[f_{\text{CM-cell}}] \nabla E_{\text{rms}}^2 / \mu$  for yeasts, as obtained in Sect. 2. The yeasts have much larger dimensions compared to the

**Fig. 3** At 10 MHz and  $\sigma_{\text{medium}} = 0.025 \text{ S/m}$ , both yeast and bacteria demonstrated positive DEP response: **a** most bacteria were trapped at the tip region of the first microelectrode pair due to their small dimensions, **b** in contrast, most yeasts were trapped at the entrance region of the first microelectrode pair even before reaching the tips, **c** on this basis, bacteria and yeasts were trapped at different locations of the microelectrode and could be separated at 10 MHz, and **d** the areas covered by yeasts (*continuous line*) and bacteria (*dashed line*) with respect to electric field contours at the bottom surface of the microchannel



bacteria, and therefore reacted more rapidly to the DEP field. This led to the immediate trapping of yeasts at the entrance region of the microelectrode before reaching the tips (Fig. 3b).

Applying a mixed suspension of bacteria and yeasts to the system, superpositioned the phenomena observed in Fig. 3a and b. While the yeasts were distinctly trapped at the entrance region of the first microelectrode pair, the bacteria were trapped at the tips (Fig. 3c). The remaining yeasts were trapped at the free ends of bacterial chains. Interestingly, the trapping region of yeasts was more restricted towards the entrance region of the microelectrode. For comparison, in

Fig. 3b, the edge of the dense mass of immobilised yeasts was  $\sim 333 \mu\text{m}$  away from the tips, whereas in Fig. 3c this distance increased to  $\sim 522 \mu\text{m}$ . This is because strong electric fields and consequently DEP forces were induced at the free ends of the bacterial chains, which created an array of tips along the microelectrode. This response was very similar to the situation observed in our previous work, in which we integrated carbon nanotubes to our DEP system to trap the model polystyrene particles at high frequencies (Khoshmanesh et al. 2010a). However, in that work we preassembled the carbon nanotubes and then applied the suspension of polystyrene particles, whereas here we

applied the bacteria and yeasts at the same time. Moreover, while a few yeasts were trapped along the outer edges of the microelectrode in Fig. 3b, no yeasts were trapped at those regions in Fig. 3c, as most of them were immobilised at the entrance region. Figure 3d shows the areas covered by yeasts (continuous line) and bacteria (dashed line) with respect to the contours of the electric field at the bottom surface of the microchannel obtained by numerical simulation (Khoshmanesh et al. 2010b).

The trapping efficiency of the DEP system was quantified by counting the number of yeasts and bacteria at the inlet and outlet of the device using a hemocytometer, as explained in Sect. 3.5. Using this technique, we obtained the trapping efficiencies of  $93.2 \pm 2.5$  and  $89.4 \pm 1.7\%$  for yeasts and bacteria, respectively.

Furthermore, we characterised the performance of the system by varying the flow rate of the sample while applying the same AC signal. At lower flow rates of  $0.3\text{--}0.7 \mu\text{lit}/\text{min}$ , the drag force was so weak that most of the yeasts and bacteria were trapped at the entrance region of the first microelectrode with yeasts distinguishably formed pearl chains between the microelectrodes (Fig. 4a). At medium flow rates of  $0.7\text{--}1.2 \mu\text{lit}/\text{min}$ , the drag force was strong enough to push most the bacteria towards the tip region, while the yeasts were trapped at the entrance region of the first microelectrode (Fig. 4b). At higher flow rates of  $1.2\text{--}1.8 \mu\text{lit}/\text{min}$ , the drag force was so strong that the yeasts were pushed towards the tip region and enclosed between the bacteria patterned along the microelectrodes (Fig. 4c).

#### 4.2 Separation of bacteria from yeasts at 100 kHz

At 100 kHz, the bacteria demonstrated positive DEP response while yeasts demonstrated negative DEP response (Fig. 1). Again, to understand the mechanism of separation, we first analysed the DEP response of bacteria (Fig. 5a) and yeasts (Fig. 5b) in separate experiments.

The bacteria were trapped at the microelectrodes, as described in Sect. 4.1. However, the density of bacterial chains grown along the microelectrode decreased and most of them were immobilised at the tip region. The bacterial chains became thicker and shorter, which indicated that the suspended bacteria were attracted towards the microelectrode edges rather than the free ends of bacterial chains (Fig. 5a). According to our experiments, a further decrease of frequency reduced the trapping region of the microelectrode and led to the accumulation of bacteria on the surface of microelectrodes, which was invisible due to the application of an inverted microscope.

Conversely, the yeasts were repelled from the microelectrodes. The yeasts that were moving far from the centreline managed to pass over the microelectrode surface

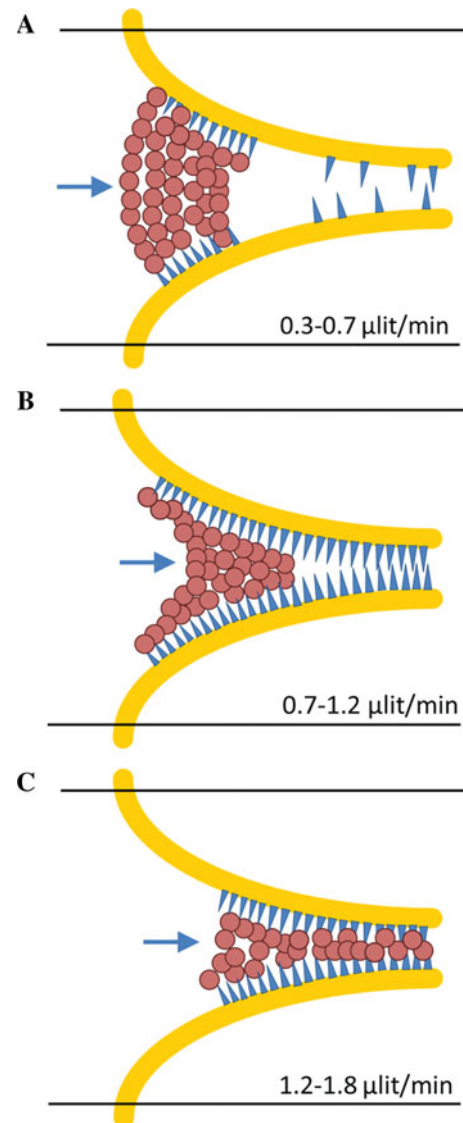
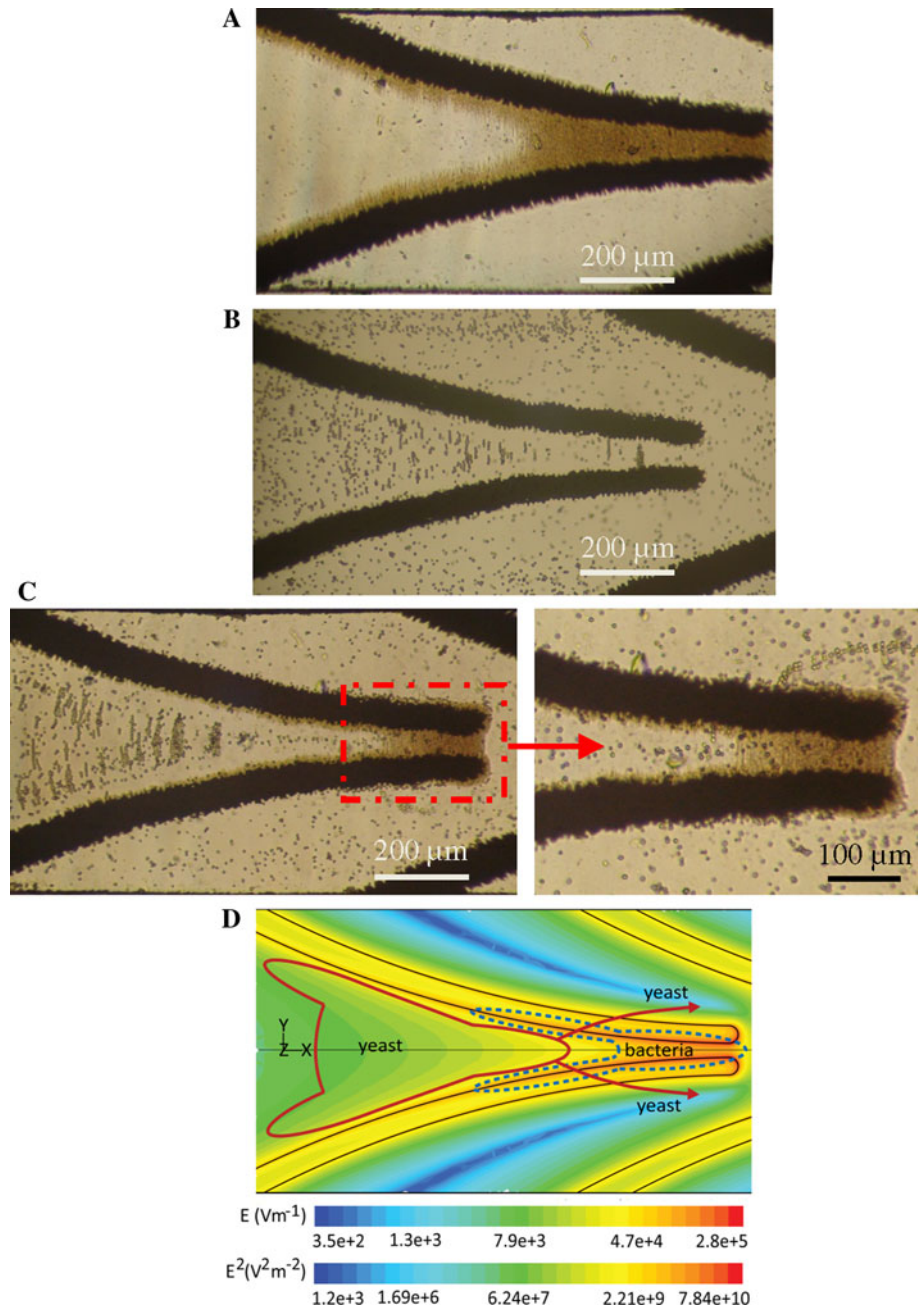


**Fig. 4** Configuration of yeasts and bacteria at different flow rates while applying an AC signal of 15 V<sub>p-p</sub> and 10 MHz: **a** low flow rate of  $0.3\text{--}0.7 \mu\text{lit}/\text{min}$ , **b** medium flow rate of  $0.7\text{--}1.2 \mu\text{lit}/\text{min}$ , and **c** high flow rate of  $1.2\text{--}1.8 \mu\text{lit}/\text{min}$

under the hydrodynamic drag force. However, the yeasts that were close to the centreline were funnelled between the microelectrodes to avoid the strong electric field regions along the edges. Accordingly, the neighbouring yeasts attached to each other to form pearl chains. Approaching the tips, the pearl chains were broken and the yeast deflected towards the sidewalls and simultaneously levitated to higher heights (Fig. 5b). This behaviour was repeated at the consequential microelectrodes, and eventually two dense strips of yeasts formed along the sidewalls.

Applying a mixed suspension of bacteria and yeasts to the DEP system resulted in the separation of the bio-particles.

**Fig. 5** At 100 kHz and  $\sigma_{\text{medium}} = 0.025 \text{ S/m}$ , bacteria and yeasts demonstrate distinct DEP responses: **a** bacteria are trapped at the microelectrodes under positive dielectrophoresis, **b** yeasts are repelled from microelectrodes under negative dielectrophoresis, and **c** on this basis, bacteria and yeasts can be separated, and **d** the areas covered by yeasts (*continuous line*) and bacteria (*dashed line*) with respect to electric field contours at the bottom surface of the microchannel



While the bacteria were trapped at the tips, the yeasts were retained behind the microelectrodes before being washed away by the drag force (Fig. 5c). The separation of bioparticles at 100 kHz enables the collection of yeasts in collection chambers or microelectrode arrays patterned downstream of the microchannel for further analysis. For example, we immobilised the yeasts repelled from the microelectrodes (Fig. 5c) on the second array of microelectrodes, which were energised at 10 MHz. However, the trapping efficiency of bacteria decreases at 100 kHz in line with the decrease of  $\text{Re}[f_{\text{CM-bacteria}}]$  (Fig. 1). Moreover, applying low frequencies can result in undesired chemical

reactions at the surface of microelectrodes and impose higher transmembrane voltage on the trapped bacteria, both threatening their viability. Figure 5d shows the areas covered by yeasts (continuous line) and bacteria (dashed line) with respect to the contours of the electric field at the bottom surface of the microchannel obtained by numerical simulation (Khoshmanesh et al. 2010b).

Using hemocytometer counting, we obtained a trapping efficiency of  $84.6 \pm 2.2\%$  for bacteria, while the separation efficiency of the system was obtained as  $85.3 \pm 1.8\%$ .

Again, we assessed the performance of the system by varying the flow rate of the sample while applying the same



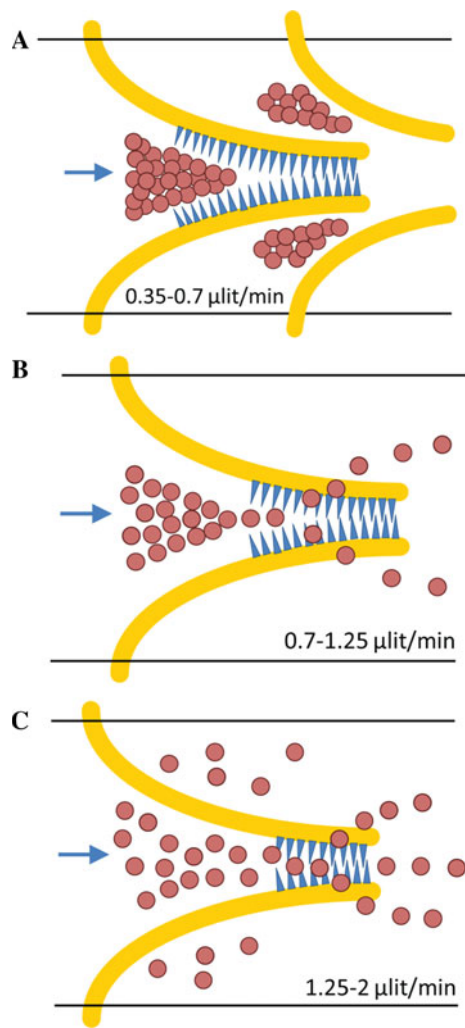


**Fig. 6** Configuration of yeasts and bacteria at different flow rates while applying an AC signal of 15 Vp-p and 100 kHz: **a** low flow rate of 0.35–0.7 µlit/min, **b** medium flow rate of 0.7–1.25 µlit/min, and **c** high flow rate of 1.25–2 µlit/min

AC signal. While the bacteria exhibited more or less similar patterns and were only pushed towards the tip region at higher flow rates, the yeasts exhibited entirely different patterns. At lower flow rates of 0.35–0.7 µlit/min, the yeasts were retained behind the microelectrodes under the repulsive DEP force and formed three distinguishable clusters between and on both sides of the first microelectrode pair (Fig. 6a). At medium flow rates of 0.7–1.25 µlit/min, the drag force was strong enough to pass the yeasts through the DEP barrier. The yeasts were funnelled between the microelectrodes and later pushed towards the sidewalls to avoid the tip region (Fig. 6b). At higher flow rates of 1.25–2 µlit/min, the yeasts which were moving close to the sidewalls were not influenced by the DEP force, while the ones close to the microchannel centreline were deflected to avoid the tips and formed three strips between and around the tips (Fig. 6c).

### 5 Conclusions

This work demonstrated the versatile capabilities of dielectrophoresis for the manipulation, separation and immobilisation of yeasts and *Lactobacillus* bacteria in microfluidic environments. The performance of the system is mainly governed by the interaction of DEP and hydrodynamic forces, which can be readily adjusted by the electrical conductivity and flow rate of the medium as well as the magnitude and frequency of AC signal applied to the microelectrodes. To characterise the response of the system, we set the first three parameters to 0.5 µlit/min, 0.025 S/m and 15 Vp-p, while changing the frequency from 10 MHz to 100 kHz. At 10 MHz, the yeasts and bacteria were trapped at different locations of the microelectrodes according to their diverse dimensions. Trapping efficiencies of  $93.2 \pm 2.5$  and  $89.4 \pm 1.7\%$  were obtained for yeasts and bacteria after a single round of sample application. At 100 kHz, the bacteria were trapped at the microelectrodes, while the yeasts were pushed towards the sidewalls and washed away by the flow. A trapping efficiency of  $84.6 \pm 2.2\%$  was obtained for bacteria, while the bio-particles were separated with a separation efficiency of  $85.3 \pm 1.8\%$  after a single round of sample application. The reported DEP-activated platform can be equipped with appropriate perfusion systems and detection mechanisms to enable the separation, immobilisation and real-time analysis of immobilised bio-particles upon exposure to different drugs and chemical stimuli.

### Appendix

Dimensions and dielectric properties of spherical yeasts, ellipsoidal yeasts and ellipsoidal *Lactobacillus* bacteria used in Fig. 1

|                              | Spherical yeasts (Huang et al. 1992) | Ellipsoidal yeasts (Huang et al. 1992) | <i>Lactobacillus</i> bacteria (Castellarnau et al. 2006) |
|------------------------------|--------------------------------------|--|--|
| External diameters (µm)      | $D = 8$                              | $D_1 = 9$<br>$D_2 = 6$                 | $D = 0.75$<br>$L = 1.5$                                  |
| Membrane thickness (nm)      | 8                                    | 8                                      | 8  |
| Wall thickness (nm)          | 220                                  | 220                                    | 50   |
| Cytoplasm conductivity (S/m) | 0.2                                  | 0.2                                    | 0.48   |
| Cytoplasm permittivity (F/m) | $50\epsilon_0$                       | $50\epsilon_0$                         | $50\epsilon_0$   |
| Membrane conductivity (S/m)  | $25 \times 10^{-8}$                  | $25 \times 10^{-8}$                    | $259 \times 10^{-6}$                                     |
| Membrane permittivity (F/m)  | $6\epsilon_0$                        | $6\epsilon_0$                          | $9.8\epsilon_0$  |
| Wall conductivity (S/m)      | $14 \times 10^{-3}$                  | $14 \times 10^{-3}$                    | $58 \times 10^{-3}$                                      |
| Wall permittivity (F/m)      | $60\epsilon_0$                       | $60\epsilon_0$                         | $78\epsilon_0$   |

## References

- Bercovici M, Kaigala GV, Mach KE, Han CM, Liao JC, Santiago JG (2011) Rapid detection of urinary tract infections using isotachopheresis and molecular beacons. *Anal Chem* 83:4110–4117
- Castellarnau M, Errachid A, Madrid C, Juarez A, Samitier J (2006) Dielectrophoresis as a tool to characterize and differentiate isogenic mutants of *Escherichia coli*. *Biophys J* 91:3937–3945
- Cho YK, Kim S, Lee K, Park C, Lee JG, Ko C (2009) Bacteria concentration using a membrane type insulator-based dielectrophoresis in a plastic chip. *Electrophoresis* 30:3153–3159
- del Carmen Jaramillo M, Torrents E, Martinez-Duarte R, Madou MJ, Juarez A (2010) On-line separation of bacterial cells by carbon-electrode dielectrophoresis. *Electrophoresis* 31:2921–2928
- Gascoyne PRC, Wang XB, Huang Y, Becker FF (1997) Dielectrophoretic separation of cancer cells from blood. *IEEE T Ind Appl* 33:670–678
- Hu XY, Bessette PH, Qian JR, Meinhardt CD, Daugherty PS, Soh HT (2005) Marker-specific sorting of rare cells using dielectrophoresis. *Proc Natl Acad Sci USA* 102:15757–15761
- Huang Y, Holzel R, Pethig R, Wang XB (1992) Differences in the AC electrodynamic of viable and non-viable yeast cells determined through combined dielectrophoresis and electrorotation studies. *Phys Med Biol* 37:1499–1517
- Kang YJ, Li DQ (2009) Electrokinetic motion of particles and cells in microchannels. *Microfluid Nanofluid* 6:431–460
- Kang YJ, Li DQ, Kalams SA, Eid JE (2008) DC-Dielectrophoretic separation of biological cells by size. *Biomed Microdevices* 10:243–249
- Khoshmanesh K, Zhang C, Nahavandi S, Tovar-Lopez FJ, Baratchi S, Hu Z, Mitchell A, Kalantar-zadeh K (2010a) Particle trapping using dielectrophoretically patterned carbon nanotubes. *Electrophoresis* 31:1366–1375
- Khoshmanesh K, Zhang C, Tovar-Lopez FJ, Nahavandi S, Baratchi S, Mitchell A, Kalantar-Zadeh K (2010b) Dielectrophoretic-activated cell sorter based on curved microelectrodes. *Microfluid Nanofluid* 9:411–426
- Khoshmanesh K, Akagi J, Nahavandi S, Skommer J, Baratchi S, Cooper JM, Kalantar-zadeh K, Williams DE, Wlodkovic D (2011a) Dynamic analysis of drug-induced cytotoxicity using chip-based dielectrophoretic cell immobilization technology. *Anal Chem* 83:2133–2144
- Khoshmanesh K, Nahavandi S, Baratchi S, Mitchell A, Kalantar-zadeh K (2011b) Dielectrophoretic platforms for bio-microfluidic systems. *Biosens Bioelectron* 26:1800–1814
- Khoshmanesh K, Kiss N, Nahavandi S, Evans CW, Cooper JM, Williams DE, Wlodkovic D (2011c) Trapping and imaging of micron-sized embryos using dielectrophoresis. *Electrophoresis* (in press). doi:10.1002/elps.201100160
- Koo OK, Liu YS, Shuaib S, Bhattacharya S, Ladisch MR, Bashir R, Bhunia AK (2009) Targeted capture of pathogenic bacteria using a mammalian cell receptor coupled with dielectrophoresis on a biochip. *Anal Chem* 81:3094–3101
- Lapizco-Encinas BH, Simmons BA, Cummings EB, Fintschenko Y (2004) Dielectrophoretic concentration and separation of live and dead bacteria in an array of insulators. *Anal Chem* 76:1571–1579
- Li H, Bashir R (2002) Dielectrophoretic separation and manipulation of live and heat-treated cells of *Listeria* on microfabricated devices with interdigitated electrodes. *Sens Actuat B Chem* 86:215–221
- Mach AJ, Di Carlo D (2010) Continuous scalable blood filtration device using inertial microfluidics. *Biotechnol Bioeng* 107:302–311
- Markx GH, Dyda PA, Pethig R (1996) Dielectrophoretic separation of bacteria using a conductivity gradient. *J Biotechnol* 51:175–180
- Mazumdar SD, Barlen B, Kaempfer P, Keusgen M (2010) Surface plasmon resonance (SPR) as a rapid tool for serotyping of *Salmonella*. *Biosens Bioelectron* 25:967–971
- Moon HS, Nam YW, Park JC, Jung HI (2009) Dielectrophoretic separation of airborne microbes and dust particles using a microfluidic channel for real-time bioaerosol monitoring. *Environ Sci Technol* 43:5857–5863
- Moschallski M, Hausmann M, Posch A, Paulus A, Kunz N, Duong TT, Angres B, Fuchsberger K, Steuer H, Stoll D, Werner S, Hagemeyer B, Stelzle M (2010) MicroPrep: chip-based dielectrophoretic purification of mitochondria. *Electrophoresis* 31:2655–2663
- Park K, Akin D, Bashir R (2007) Electrical capture and lysis of vaccinia virus particles using silicon nano-scale probe array. *Biomed Microdevices* 9:877–883
- Persat A, Santiago JG (2011) MicroRNA profiling by simultaneous selective isotachopheresis and hybridization with molecular beacons. *Anal Chem* 83:2310–2316
- Pethig R (2010) Review article-dielectrophoresis: status of the theory, technology, and applications. *Biomicrofluidics* 4:022811
- Qiu J, Zhou Y, Chen H, Lin J-M (2009) Immunomagnetic separation and rapid detection of bacteria using bioluminescence and microfluidics. *Talanta* 79:787–795
- Treuer R, Haydel SE (2011) Acid-fast staining and Petroff-Hausser chamber counting of mycobacterial cells in liquid suspension. *Curr Prot Microbiol*, Chap 10:10A.16.11–10A.16.16
- Wang XB, Huang Y, Burt JPH, Markx GH, Pethig R (1993) Selective dielectrophoretic confinement of bioparticles in potential-energy wells. *J Phys D Appl Phys* 26:1278–1285
- Xia N, Hunt TP, Mayers BT, Alsberg E, Whitesides GM, Westervelt RM, Ingber DE (2006) Combined microfluidic-micromagnetic separation of living cells in continuous flow. *Biomed Microdevices* 8:299–308
- Yang L (2008) Electrical impedance spectroscopy for detection of bacterial cells in suspensions using interdigitated microelectrodes. *Talanta* 74:1621–1629
- Zhou RH, Wang P, Chang HC (2006) Bacteria capture, concentration and detection by alternating current dielectrophoresis and self-assembly of dispersed single-wall carbon nanotubes. *Electrophoresis* 27:1376–1385